THEORETICAL SHOCK-LAYER PLASMA FLOW PROPERTIES FOR THE SLENDER PROBE AND COMPARISON WITH THE FLIGHT RESULTS

By Paul W. Huber and John S. Evans

NASA Langley Research Center
Langley Station, Hampton, Va.

For Presentation at Second Symposium on
the Plasma Sheath

Boston, Massachusetts
April 10-12, 1962

UNCLASSIFIED ~~CONFIDENTIAL~~

THEORETICAL SHOCK-LAYER PLASMA FLOW PROPERTIES FOR THE SLENDER PROBE AND COMPARISON WITH THE FLIGHT RESULTS

By Paul W. Huber* and John S. Evans*

ABSTRACT

The VHF attenuation measured at two locations on the body during flight at 17,700 ft/sec is compared to theoretical values computed on the basis of equilibrium, nonequilibrium, inviscid- and viscous-flow models. The shock-layer plasma-flow computational procedure included modification of the inviscid-flow properties near the body surface for the effects due to boundary-layer flow, and application of nonequilibrium concepts to the flow along streamlines. Attenuation is computed on the basis of plane-wave transmission at normal incidence through a nonuniform plasma layer. Comparison of the resulting theoretical attenuations with the flight measurements clearly points up the importance of the non-equilibrium and viscous-flow aspects of the plasma-sheath flow. Also discussed are some aspects of the wave-plasma transmission model used.

*Aerospace Technologist.

L-3002

UNCLASSIFIED ~~CONFIDENTIAL~~

UNCLASSIFIED CONFIDENTIAL

THEORETICAL SHOCK-LAYER PLASMA FLOW PROPERTIES

FOR THE SLENDER PROBE AND COMPARISON

WITH THE FLIGHT RESULTS

By Paul W. Huber* and John S. Evans*

NASA Langley Research Center

INTRODUCTION

Existing theoretical approaches to the description of hypersonic blunt-body plasma sheaths are generally inadequate because of the difficulty of handling the interplay between viscous and nonequilibrium effects. Since the R-F signal loss through the sheath is strongly dependent upon the magnitude and distribution of plasma properties, an experimental approach to the radio blackout problem is indicated and indeed is being pursued by various groups. It is hoped that the results from these programs will supply numbers for use in design of radio-link systems. A more important result might be that such numbers will serve to establish the usefulness of theoretical approximations which can be applied to the development of advanced design concepts.

The recent flight results of the RAM vehicles have provided the first numbers obtained under maximum attenuation flight conditions and with specifiable flight conditions and are proving to be of great value for providing a better understanding of the nature of the problem. These flight results will be compared to the results of a first-order theoretical

*Aerospace Technologist.

approach to the problem. For expediency, this comparison is to be made at only one point on the flight trajectory. Referring to figure 1, this is the point of maximum signal loss from the two VHF antennas and corresponds to flight at an altitude of about 170,000 feet and a velocity of 17,700 feet per second.

THEORETICAL APPROACH

Since time will not permit a detailed description of the computational method, the general approach will be outlined and the ground rules governing the procedure will be discussed briefly. For this purpose a schematic representation of the shock-layer-flow model is shown in figure 2. This flow model is first constructed on the basis of equilibrium inviscid flow, and the resulting shock shape, pressure distribution, and streamline paths then serve as inputs to the subsequent steps which involve perturbation of the flow properties for boundary-layer and thermochemical nonequilibrium effects.

The equilibrium inviscid flow inputs will not be discussed since they merely represent modifications of real-gas characteristics solutions found in the literature for a hemisphere -9° cone body. These solutions were made at the General Electric Company, reference 1, and the modifications which we have made are allowances for the somewhat different altitude and Mach number of our case, and for the Prandtl-Meyer expansion which occurs at the cone-cylinder juncture in our case. These adjustments can be made using correlation parameters involving the normalized

flow coefficients and give good results if the altitude and Mach number are not greatly different. The results are given in table I.

The next step in the procedure was to apply nonequilibrium concepts to the flow along streamlines, and it was assumed that both the streamline paths and the pressure distributions along the paths are identical to the equilibrium case. Then, using the inviscid nonequilibrium flow properties along the body streamline as a basis for boundary-layer estimates, boundary-layer profiles were constructed and "matched" to inviscid flow profiles at given body normals. Inside the matching line the streamline paths were altered on the basis of continuity considerations, and nonequilibrium concepts were applied along these paths using appropriate boundary-layer-flow properties but neglecting diffusion between streamlines. Finally, electron concentration and collision frequency profiles along body normals were constructed. These two profiles are the input required for the computation of signal loss in transmitting through the plasma layer at a given point.

NONEQUILIBRIUM CONCEPTS

Upper and lower bounds for the nonequilibrium effects can reasonably be taken as corresponding to infinitely slow and infinitely fast rates for all reactions after the attainment of complete equilibrium immediately upon crossing the shock front. These upper and lower bounds are referred to as shock frozen and equilibrium, respectively, and were shown by Mr. Sims in the preceding talk. As might be expected, these

rather extreme limits bracketed the experimental values but leave a large area of uncertainty.

Closer approximations to the true plasma properties can be obtained by considering the effects of finite reaction rates. The most desirable way of doing this would be to set up a computer program which simultaneously calculates the composition, thermodynamic properties, and flow-field properties. Programs of this nature are under development by Cornell Aero. Lab., AVCO, GASL, GE, and perhaps others. In order to obtain results quickly we have elected to use methods which are less accurate but readily available.

Concurrently with our program a flow-field program was contracted to the AVCO Wilmington Lab. to calculate temperature, density, and electron concentration profiles for the same body and flight conditions. The results of the two programs are similar, although some differences were noted and will be shown later.

The determination of the effects of finite reaction rates on the flow along a streamline was carried out in two steps.

Thermal properties.- The first step involved determination of the neutral species composition and the thermal properties of the flow while neglecting ionization and ionic recombination. This procedure is justified in the RAM case, since the fraction of ionic species in the flow is too small to contribute to the thermal properties of the gas. The properties along streamlines were found, therefore, using the following chemical kinetic model: (1) vibration is in local equilibrium

with the temperature (2) dissociation of O_2 is the controlling rate in production of atoms and NO in the shock flow and expansion behind the shock.

Using this model the procedure along a streamline started at the shock where the air behind the shock was at first undissociated but in vibrational equilibrium with the high translational temperature. The two-body dissociation rate of O_2 was then applied to the flow along the streamline by an iteration technique until, at some point in the expansion of the flow, the O_2 dissociation slowed down to a very low value.

The atom fraction corresponding to the degree of dissociation attained at this point was distributed between O and N atoms in the ratio 5 to 1, which corresponds roughly to that obtained by Duff and Davidson (ref. 2) behind normal shock waves at temperatures of 7,000° K and 10,000° K. O_2 and N_2 concentrations were adjusted accordingly. The mole fractions of O, N, O_2, and N_2 thus obtained at this point were then held constant for the remainder of the streamtube expansion. The resulting temperature variation along a streamline for this case is shown in figure 3(a) and compared with the frozen-at-shock and equilibrium cases.

Ionization.- At the freeze point for neutral species all the ionization reactions were assumed to be in local equilibrium. In the expansion subsequent to this freeze point no three-body recombination of ions was permitted. Thus the finite rate adjustment of electron concentration

depended only on the two-body dissociative recombination of NO^+. The initial value of NO^+ at the freeze point was evaluated using the concentrations of N and O and the equilibrium constant $K = \frac{(NO^+)(e^-)}{(N)\,(O)}$. The subsequent variation of NO^+ was calculated using a temperature independent value of 10^{-8} cm^3 sec^{-1} for the dissociative recombination rate as recommended by Bortner, reference 3. The decay rate of electron concentration with distance was found to vary as $\frac{1}{u}(Ne)^2$. Figure 3(b) illustrates the variation of Ne along a streamline using this model, and also shows the comparison with the limiting cases.

VISCOUS FLOW CONCEPTS

Attempts to include gross effects due to viscous shock-layer flow have been made and are, at the very best, only rough estimates. The intent of this work is to show the importance of such effects on the plasma properties, and to point up the need for a more comprehensive treatment of the problem of shock-layer plasma flow. In this regard, classical boundary-layer theory is applied even though the layers are not classically thin nor the free-stream uniform.

The boundary-layer flow parameters are found using real-gas laminar similar solutions taken from the program given by Cohen in reference 4. The solutions used are for equilibrium flow, Lewis number of one and pressure gradient of zero. The solutions are applied using the assumption that inviscid wall thermal properties are appropriate to the

boundary-layer edge. The boundary-layer profile which is thus obtained is thermally "matched" to the inviscid shock layer by an arbitrary means which is illustrated in figure 4. Here the temperature variation through the boundary layer is plotted along with that through the inviscid shock layer at a given station or normal located along the body. Generally these curves will intersect and the point of intersection then defines that point within which the boundary-layer properties are used per se, and outside of which the inviscid shock-layer properties are used. A mass-flow identification parameter, $\int_0^y \rho u \, dy$, is used to identify a "streamline" once it has come within the matching line or boundary-layer flow region. While not shown here, the viscous and inviscid velocity profiles are "matched" by simply fairing from the boundary-layer velocity to the inviscid flow velocity in the region from the wall to the boundary-layer edge (not the matching point in this case).

The nonequilibrium concepts previously discussed in connection with the inviscid flow along streamlines were also applied to the "streamline" flow within the viscous region by using the appropriate temperature, density, and velocity variation along constant $\int_0^y \rho u \, dy$ lines within this region.

WAVE PROPAGATION MODEL

The following concepts were used in the determination of signal loss through the shock-layer plasma:

(1) The incident signal was assumed to be a plane wave at normal incidence.

(2) The plasma properties were assumed to be unaffected by the passage of the signal.

(3) Plasma properties were assumed to vary only in the direction parallel to the direction of propagation. In this regard, no allowance was made for variation of plasma properties over the finite dimensions of the antennas. (For example, the plasma properties for the beacon antenna were taken to be those calculated at $\frac{x}{D_N} = 5.4$, whereas the antenna actually extended from $\frac{x}{D_N} = 3.4$ to $\frac{x}{D_N} = 7.4$.)

(4) No restriction was placed on the variation of plasma properties in the propagation direction. Any type of gradient in plasma properties was allowed, either continuous or discontinuous in nature.

The amplitude of the signal transmitted through the plasma was found by numerical integration of the propagation equation shown in figure 5. The solutions were obtained using the Runge-Kutta method on an IBM 7090 computer. The resulting ratio of transmitted power to incident power was converted to signal loss in decibels, as was the ratio of reflected to incident power.

RESULTS AND DISCUSSION

From plots of the results of the shock-layer plasma computation electron concentration and collision frequency variation along a body normal were tabulated for the electronic computer, which then calculated the signal loss and reflection for R-F propagation through the plasma. A typical case is shown in figure 6. By repeating this procedure at a number of points along the body, the signal loss variation with distance along the body was determined. These results are shown in figure 7 and are compared with the experimental values of VHF signal loss for the beacon and the telemeter antennas at the maximum attenuation point in the RAM flight. Also shown for comparison are the results of the limiting plasma-flow models which were shown in the previous talk.

The curve shown passing between the experimental points is the one for which both finite reaction rates and viscous effects were considered. The term "frozen-downstream" refers to the fact that, due to finite-rate oxygen dissociation, the composition was frozen at a point downstream of the shock rather than frozen at the shock as was assumed for the upper limit. The term "finite-rate" indicates that dissociative recombination of NO^+ ions reduces electron concentration in the flow following the freeze point. The letters "B-L" indicate that viscous effects are included in the estimate. It is seen that this estimate falls roughly midway between the limiting cases of frozen-at-shock and equilibrium.

The curve labeled frozen-downstream is intended to show the effects due to finite-rate oxygen dissociation. It was . und in the computation of this case that the freeze point for the body streamline was at about the stagnation point, and that for the outer streamlines this freeze point occurs farther back towards the nose-cone juncture region. The effects of finite-rate NO^+ recombination and viscosity are then seen by comparison of these two curves, that is, the F-D with the F-D, F-R, B-L.

In order to illustrate the effects due to boundary-layer growth, the curve labeled "equilibrium-B-L" is shown. For this case, it is seen that the B-L essentially washes out the attenuation, due to the cooling of the plasma layer near the surface. It might be mentioned also that there was no temperature peak in the equilibrium B-L profile, but that in the case of the frozen-downstream thermal boundary layer, a peak did occur.

The AVCO results mentioned previously have been converted to attenuation using our wave propagation program, and are shown on the figure as symbols. There are seen to be some differences in the results. It might be pointed out that one difference in the two programs was the inclusion of the atomic ionization reactions in our program. It was found, however, that these effects were of no importance in this case. Another difference in the programs was the inclusion of electron overshoot in the AVCO program, and this may account for the higher attenuation at $\frac{x}{D_N} = 0.42$ of the AVCO result.

The signal loss due to reflection from the plasma is shown in figure 8 for the same cases as shown for the total signal loss in figure 7. The reflection losses are seen to be, generally, a substantial fraction of the total losses. It is also seen that for the finite-rate and frozen cases reflection accounts for a much larger fraction of the total than in the equilibrium cases. This result, of course, is due mainly to the higher ratio of N_e to critical N_e in the aforementioned cases.

In general, it can be concluded from the results shown that non-equilibrium effects and viscous effects in the gas flow about the body are the major influences on the plasma properties which influence VHF signal attenuation. While the estimates given are too gross to accurately describe the situation, it is clear that these effects are strong and that a more comprehensive theoretical treatment of the problem is indicated and necessary before future design concepts of signal-link systems can be firmly established.

REFERENCES

1. FitzGibbon, Sheila A.: Real Gas Supersonic Flow Field Solutions in the Shock Layer Around a 9° Sphere-Cone at Mach = 20.4, 21.4, and 21.2. G.E. Co. MSVD; Aero. Data Memo No. 1:48, May 1961.
2. Duff, Russell E., and Davidson, Norman: Calculation of Reaction Profiles Behind Steady State Shock Waves. II. The Dissociation of Air. Jour. Chem. Phys., Vol. 31, No. 4, pp. 1018-1027 (Oct. 1959).
3. Bortner, M. H., and Baulknight, C. W.: Deionization Rates. Final Report on Contract No. AF 19(604)-7273; AFCRL 320, April 28, 1961.
4. Cohen, Nathaniel B.: Boundary-Layer Similar Solutions and Correlation Equations for Laminar Heat-Transfer Distribution in Equilibrium Air at Velocities up to 41,100 Feet Per Second. NASA TR R-118, 1961.

TABLE I.- INPUT DATA FOR SHOCK-LAYER PLASMA DETERMINATION

[Modification of data taken from ref. 1]

	Shock		Body	No. 1 streamline		No. 2 streamline		Remarks
$\frac{x}{D_N}$	$\frac{\Delta}{D_N}$	$\frac{p_{sh} - p_1}{p_2 - p_1}$	$\frac{p_b - p_1}{p_2 - p_1}$	$\frac{p - p_1}{p_2 - p_1}$	$\frac{y}{D_N}$	$\frac{p - p_1}{p_2 - p_1}$	$\frac{y}{D_N}$	
0	0.030	1.00	1.042	------	------	------	------	Normal shock and stagnation point
0.42	0.180	0.325	0.075	0.112	0.0558	0.156	0.097	Hemi-cone juncture
1.0	0.331	0.112	0.038	0.038	0.0867	0.040	0.1461	
2.0	0.485	0.065	0.026	0.026	0.0849	0.026	0.154	
5.4	0.662	0.030	0.0185	0.0185	0.0649	0.0185	0.121	Center line of the beacon slot antenna
11.5	0.715	0.0167	0.0194 .0084	0.0194	0.0336	0.0194	0.0858	Cone-cylinder juncture
16	1.470	0.0135	0.0093	0.0093	0.0500	0.0093	0.125	Telemeter ring antenna

See figure 2 for coordinate system.

p_{sh} = Shock pressure

p_b = Body pressure

p_2 = Normal shock pressure

p_1 = Ambient flight pressure

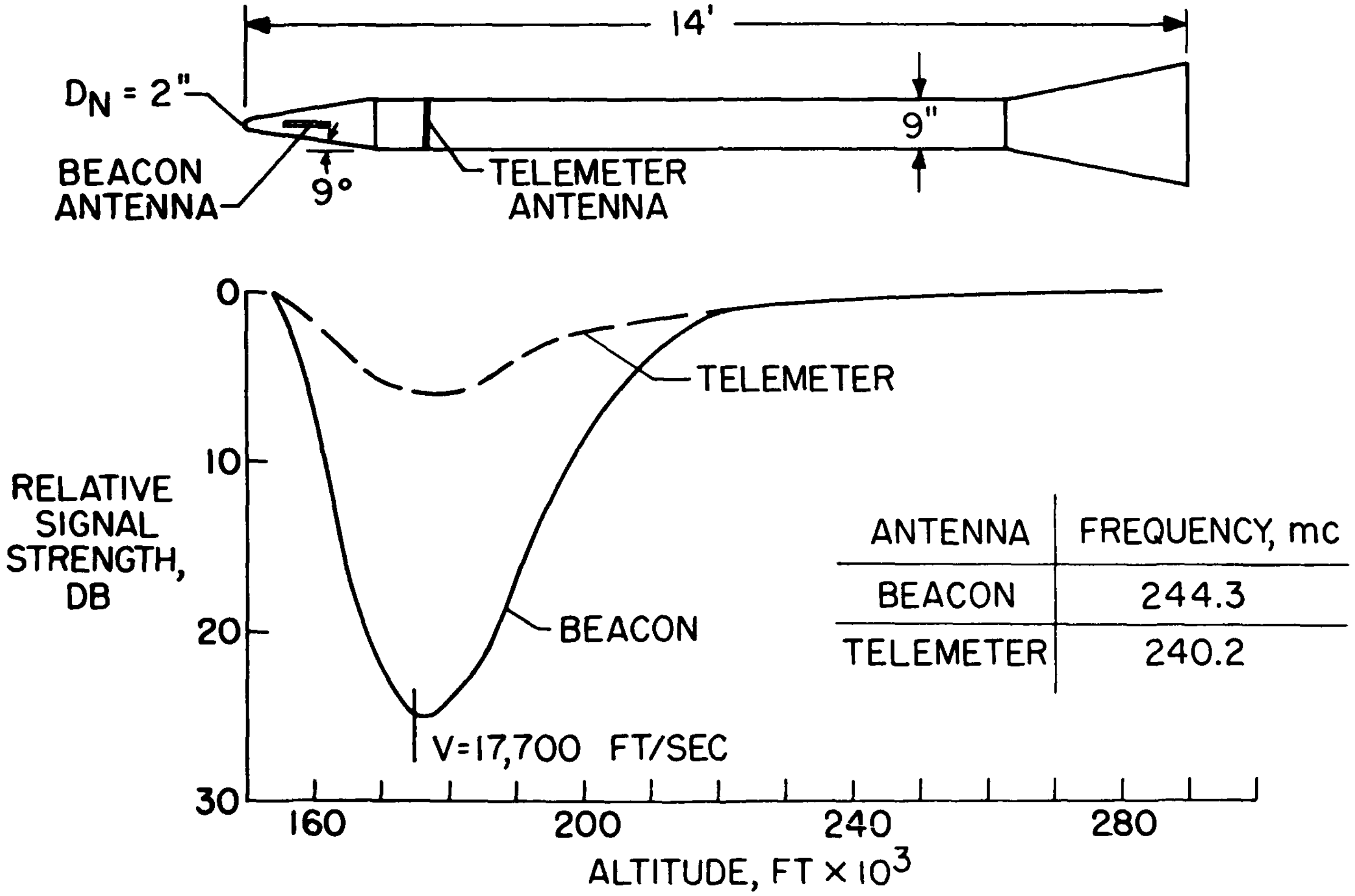

NASA

Figure 1.- Experimental signal loss for RAM-A1 reentry.

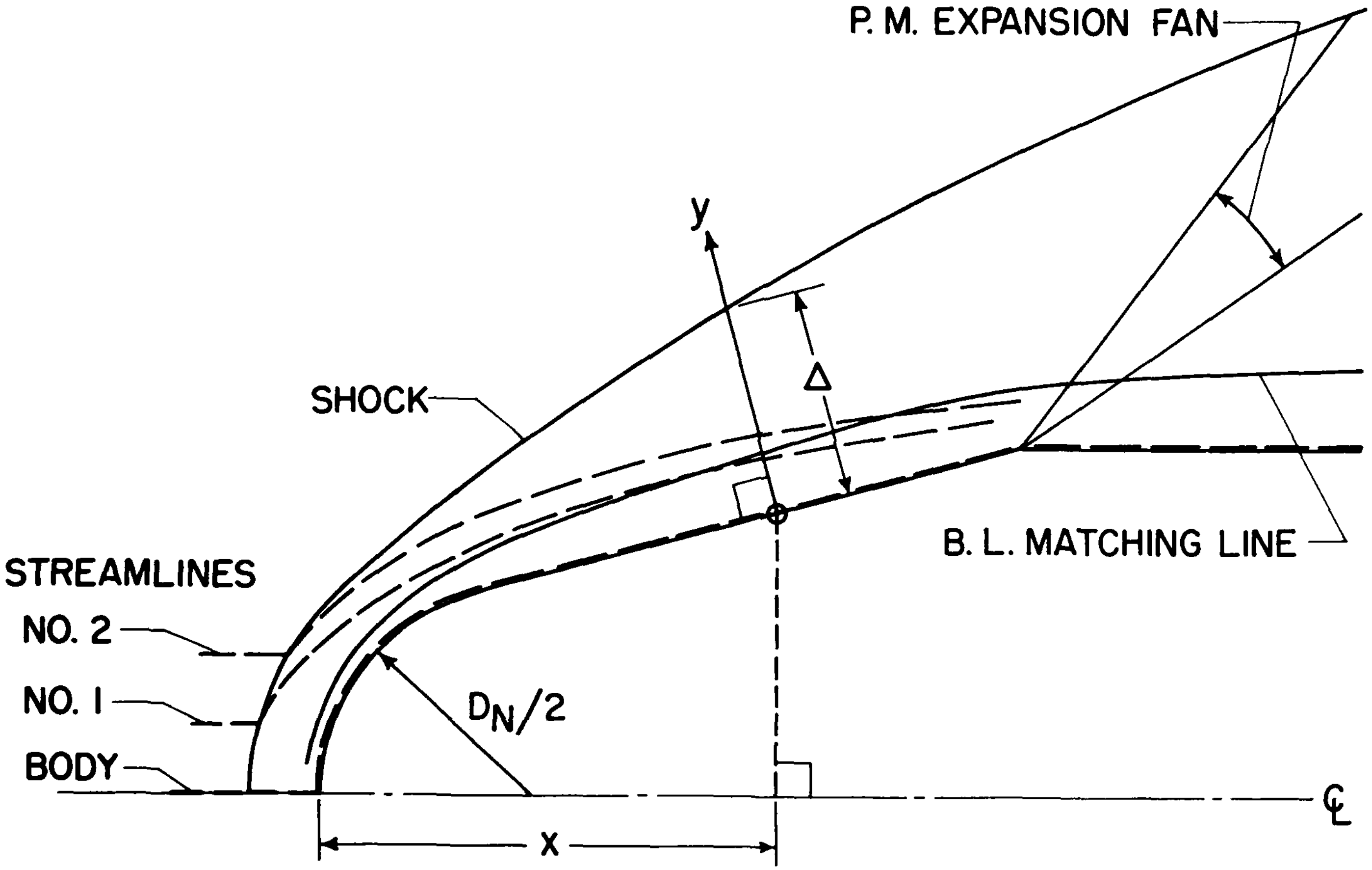

NASA

Figure 2.- Shock-layer flow model for RAM-A1 plasma description.

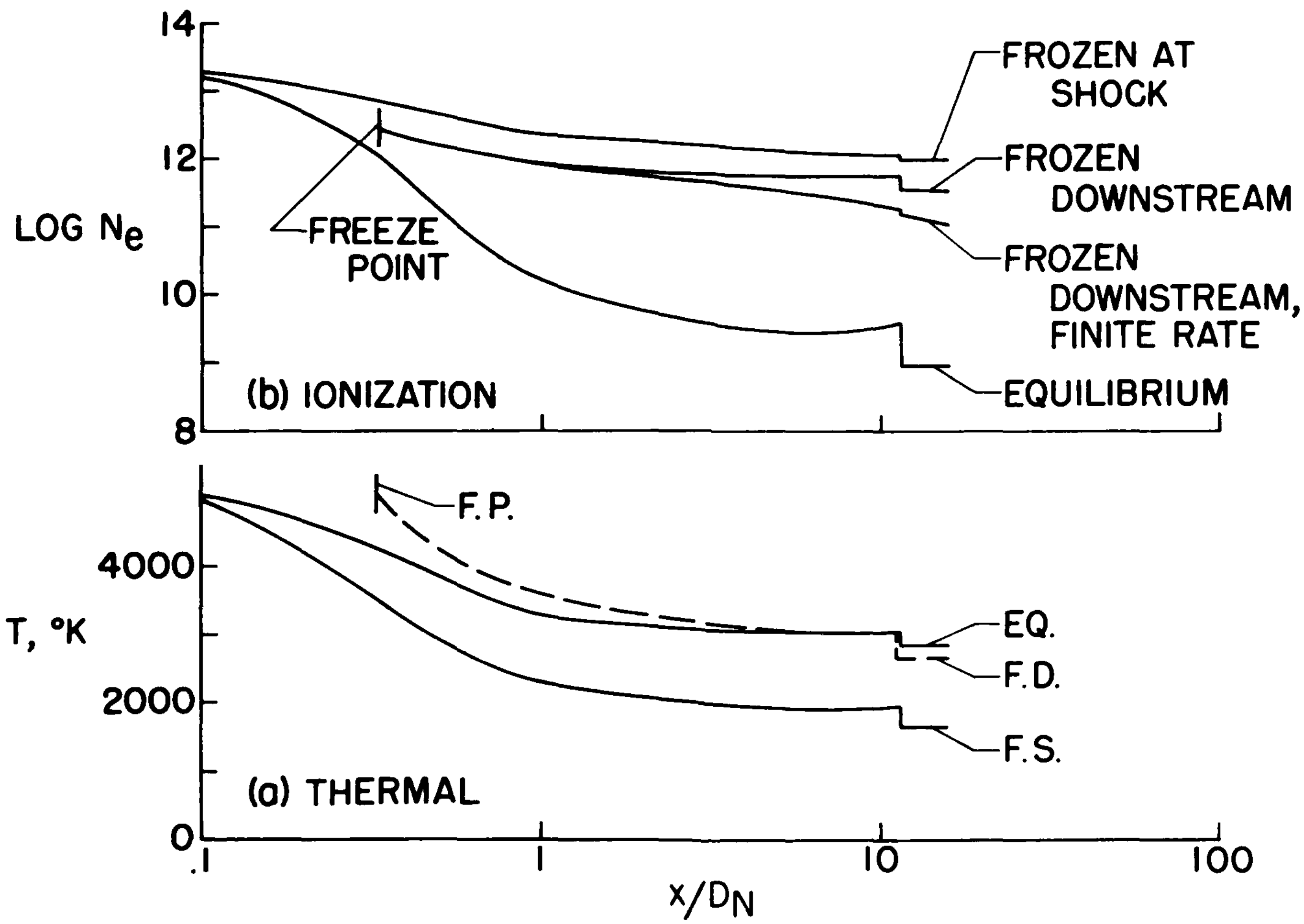

NASA

Figure 3.- Effects of nonequilibrium on properties along streamline no. 1.

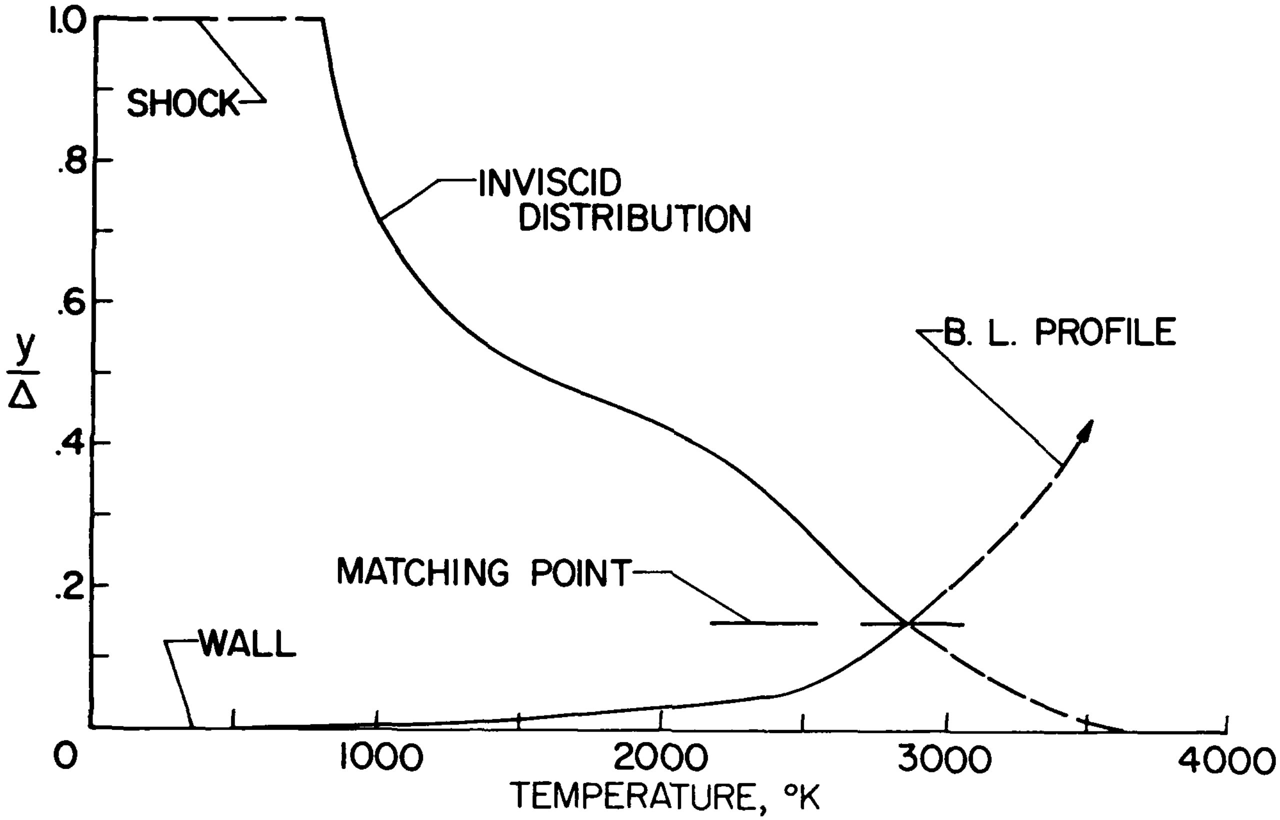

NASA

Figure 4.- Illustration of boundary-layer matching procedure, $x/D_N = 5.4$ (beacon antenna), equilibrium flow.

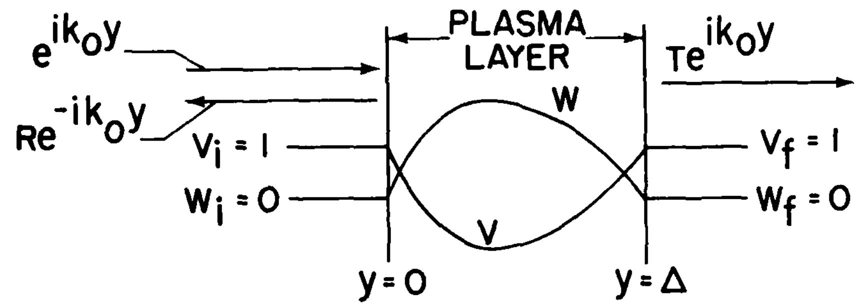

$$\frac{d^2E}{dy^2} + k^2E = 0, \quad E = r + is, \quad k^2 = k_o^2\,[V + iW]$$

$$\frac{d^2r}{dy^2} + k_o^2\,[rV - sW] = 0, \quad \frac{d^2s}{dy^2} + k_o^2\,[sV + rW] = 0$$

$$V = 1 - \frac{1}{\left(\frac{\nu}{\omega_p}\right)^2 + \left(\frac{\omega}{\omega_p}\right)^2} \qquad W = \frac{\nu/\omega_p}{\omega/\omega_p}\left[\frac{1}{\left(\frac{\nu}{\omega_p}\right)^2 + \left(\frac{\omega}{\omega_p}\right)^2}\right]$$

ω_p = PLASMA FREQUENCY	E = ELECTRIC FIELD INTENSITY
ω = SIGNAL FREQUENCY	k = PROPAGATION PARAMETER
ν = COLLISION FREQUENCY	

NASA

Figure 5.- Equations for signal propagation through a nonuniform plasma layer.

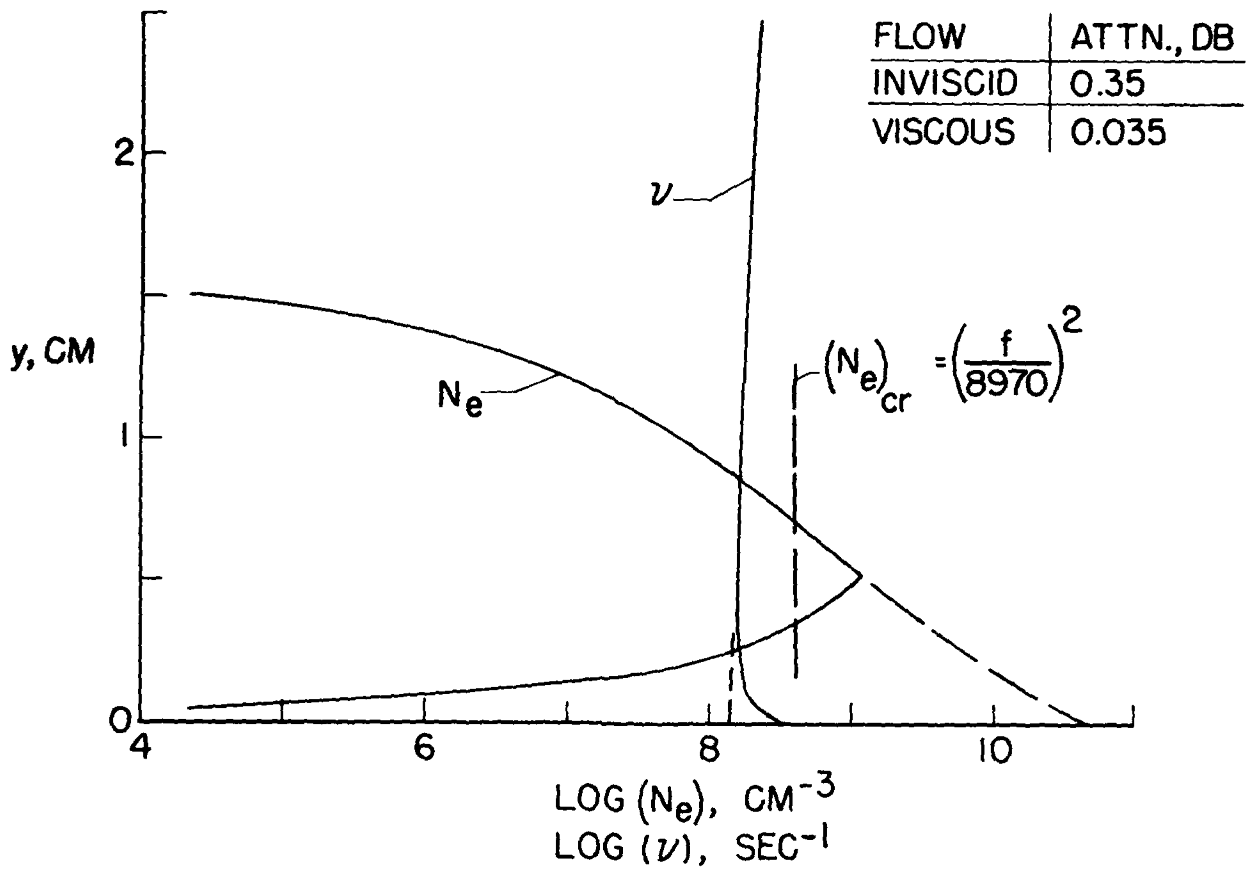

NASA

Figure 6.- N_e and ν in shock layer for equilibrium flow, $x/D_N = 5.4$.

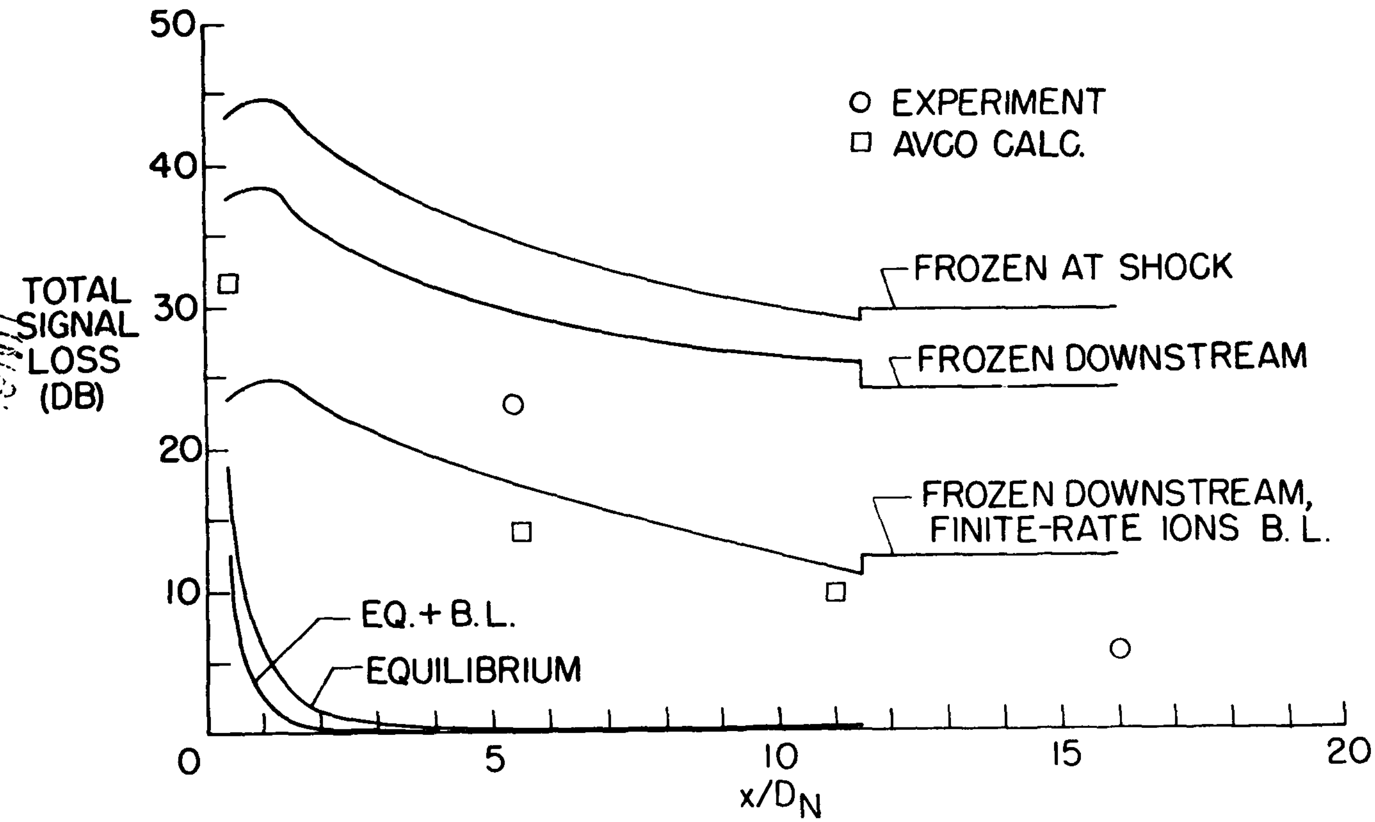

NASA

Figure 7.- Total attenuation for some shock-layer plasma flow models.

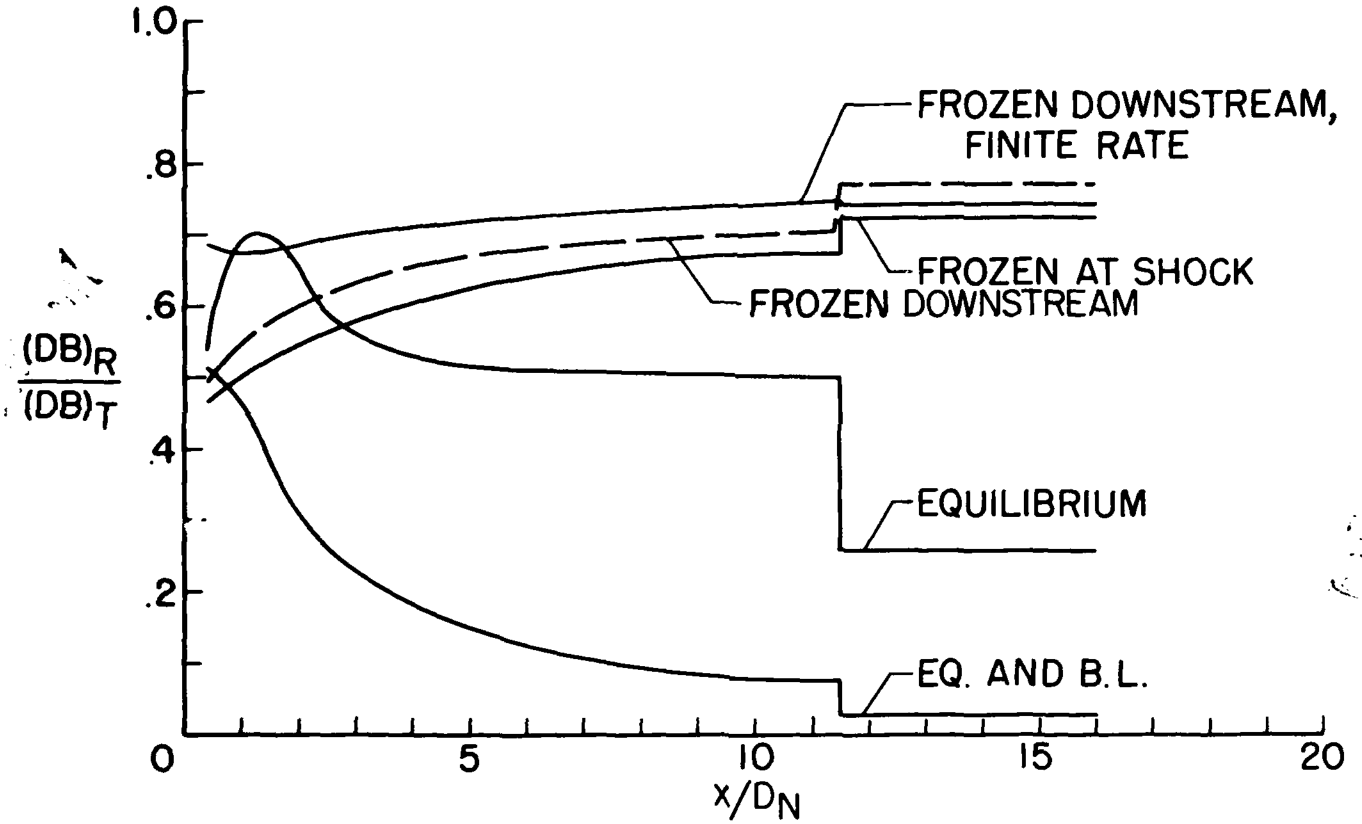

NASA

Figure 8.- Ratio of signal loss due to reflection to total signal loss.